The interaction of interface optical phonons with an electron in an asymmetric quantum well

1992 J. Phys.: Condens. Matter 4 9769

(http://iopscience.iop.org/0953-8984/4/49/005)

J. Phys.: Condens. Matter 4 (1992) 9769–9778. Printed in the UK

The interaction of interface optical phonons with an electron in an asymmetric quantum well

Xi Xia Liang

CCAST (World Laboratory), PO Box 8730, Beijing 100080, People's Republic of China and Laboratory of Solid State Physics, Department of Physics, Neimenggu University, Hohhot, Neimenggu 010021, People's Republic of China†

Received 4 February 1992, in final form 17 July 1992

Abstract. Long-wavelength optical modes of lattice vibrations are studied and a Fröhlich-like Hamiltonian of the interaction between an electron and the interface optical phonons is derived. Interesting properties of the interface optical modes and their coupling with electrons are found. The numerical results for the dispersion relations, eigenvectors and coupling functions of the interface optical phonons in several practical systems are obtained and discussed. It is shown that the interface optical modes should be taken into consideration in theoretical investigations of electron–phonon scattering in heterostructures.

1. Introduction

In recent years, much attention has been paid to the electron–optical-phonon interaction in semiconductor heterostructures [1–13]. Raman scattering measurements for semiconductor quantum wells have shown that a transverse vibration occurs at the bulk longitudinal optical (LO) frequency, while a longitudinal mode occurs at the bulk transverse optical (TO) frequency [2]. The polaron effects at frequencies lower than the usual LO frequencies are found by cyclotron resonance (CR) and magnetophonon resonance (MR) observations [3–5]. These phenomena are somewhat surprising and various theoretical explanations have been proposed [2, 6–9]. An interface-mode mechanism has been suggested [4, 7, 8]. Some authors have studied theoretically the properties of the electron–optical-phonon interaction in polar semiconductor heterostructures such as the single heterojunction and symmetric double heterostructures [11–13]. It is shown that the optical vibration modes can be strongly influenced by the presence of heterointerfaces; these give rise to the appearance of new modes which are localized in the vicinities of interfaces and can be called interface optical (IO) modes. A detailed study of IO phonons and their coupling with electrons in various systems of heterostructures is necessary.

In this paper a general situation, the asymmetric quantum well, is considered. The optical modes of lattice vibrations are first determined within the framework of the dielectric continuum model [13–16] and then an implied dispersion relation and the eigenvectors for the IO modes are given in section 2. A Fröhlich-like Hamiltonian describing the electron–IO-phonon interaction in the system is derived in section 3.

† Mailing address.

0953-8984/92/499769+10$07.50

The properties of these modes and corresponding electron–phonon coupling are qualitatively analysed in section 4. In some special cases our results can be reduced to those for symmetric double heterostructures [11, 13], the single heterojunction [12] and an isolated slab [17] etc. Numerical calculations for several practical systems are carried out and discussed in section 5. It turns out that the effects of interface modes may contribute to electron–phonon scattering in heterostructures.

2. Interface optical modes

We consider a system whose geometry is shown in figure 1. The well material 1 lies in the region I ($|z| \leqslant d$) and the barrier materials 2 and 3 fill up the spaces II ($z > d$) and III ($z < -d$) respectively. A similar system has been considered in studying the surface polaritons, the modes of coupled photons and dipole excitations of the solid [10]. We now start from a microscopic consideration of the optical vibrations of lattices in order to deal with the electron–phonon interaction problem. In the dielectric continuum model, the relative displacement $\boldsymbol{u}(\boldsymbol{r}, t)$ of the ion pair at $\boldsymbol{r}$ in a diatomic polar crystal satisfies the following equation of motion:

$$\mu\ddot{\boldsymbol{u}}(\boldsymbol{r}, t) = -\mu\omega_0^2\boldsymbol{u}(\boldsymbol{r}, t) + e^*\boldsymbol{E}^{\mathrm{l}}(\boldsymbol{r}, t) \tag{1}$$

where μ is the reduced mass of the ion pairs, ω_0 is the frequency associated with the short-range force between the ions and e^* is the effective charge of the ions. $\boldsymbol{E}^{\mathrm{l}}(\boldsymbol{r}, t)$ is the local electric field related to the polarization field $\boldsymbol{P}(\boldsymbol{r}, t)$ by

$$\boldsymbol{P}(\boldsymbol{r}, t) = ne^*\boldsymbol{u}(\boldsymbol{r}, t) + n\alpha\boldsymbol{E}^{\mathrm{l}}(\boldsymbol{r}, t) \tag{2}$$

where n and α are respectively the number of Wigner–Seitz cells per unit volume and the electric polarizability per cell. On the bases of dipolar-field and Lorentz local-field theories, we have the following integral equations for the polarization field in the region λ [13, 16, 17]:

$$\gamma_j^\lambda P_j^\lambda(\boldsymbol{r}, t) = \sum_{\lambda' l} \int_{(\lambda')} T_{jl}(\boldsymbol{r} - \boldsymbol{r}') P_l^{\lambda'}(\boldsymbol{r}', t)\, \mathrm{d}\boldsymbol{r}. \tag{3}$$

In equation (3) $\lambda, \lambda' =$ I, II or III label the regions and $l, j = x, y$ or z. The integral is over the region λ'. T_{jl} is the dipolar tensor [16, 17]. γ_j^λ is determined by

$$\gamma_x^\lambda = \gamma_y^\lambda = \gamma_k^\lambda = \frac{(\omega_{0\lambda}^2 - \omega^2)(1 - \frac{4}{3}\pi n_\lambda\alpha_\lambda) - \omega_{p\lambda}^2/3}{n_\lambda\alpha_\lambda(\omega_{0\lambda}^2 - \omega^2) + \omega_{p\lambda}^2/4\pi} \tag{4}$$

$$\gamma_z^\lambda = \gamma_k^\lambda + 4\pi. \tag{5}$$

Carrying out a two-dimensional (2D) Fourier transformation one can obtain [13]

$$\gamma_j^\lambda P_j^\lambda(\boldsymbol{k}, z) = -\frac{2\pi}{k} \sum_{\lambda'} \int_{(\lambda')} \mathrm{d}z' \sum_l K_j K_l \mathrm{e}^{-k|z-z'|} P_l^{\lambda'}(\boldsymbol{k}, z') \tag{6}$$

where

$$\boldsymbol{K} = (k, 0, \mathrm{i}k\,\mathrm{sgn}(z - z')). \tag{7}$$

k is the 2D wavenumber in the $x-y$ plane. Here the x-axis has been chosen to lie along k. The coefficient γ_k^λ can also be related to the macroscopic parameters of the materials by the equation

$$\gamma_k^\lambda = 4\pi/(\epsilon_\lambda - 1) \tag{8}$$

which is implied in the derivation from equations (2) to (3). Here the dielectric constant ϵ_λ is a function of the frequency and is given by

$$\epsilon_\lambda(\omega) = \epsilon_{\infty\lambda}(\omega_{L\lambda}^2 - \omega^2)/(\omega_{T\lambda}^2 - \omega^2). \tag{9}$$

In equation (9), $\epsilon_{\infty\lambda}$ and $\omega_{L\lambda}(\omega_{T\lambda})$ are respectively the optical dielectric constant and the bulk LO- (TO-) phonon frequency of the material $\lambda(\lambda = 1,2,3)$.

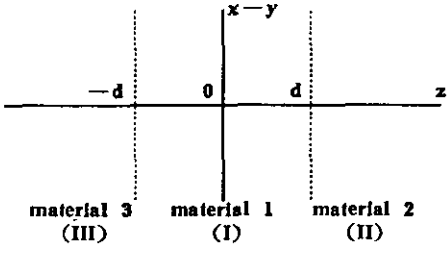

Figure 1. Geometry of the system.

Equations (6) and (7) can be discussed for the situations in which γ_j^λ is equal to zero or otherwise. For the cases of $\gamma_k^\lambda = 0$ and $\gamma_z^\lambda = 0$, we get confined bulk-like modes, TO and LO modes of the material λ, respectively. These are simply the results obtained by previous authors [15–17] for a dielectric slab. We do not plan to discuss them here.

We focus our attention on the case of $\gamma_j^\lambda \neq 0$. In this case we get extra modes. In solving equations (6) and (7), the convergence of the solutions at $z \to \pm\infty$ is applied and the boundary conditions at the interfaces are 'buried' in the system of integral equations which couple the different regions I, II and III [15–17].

The condition of compatibility for the equation system to have non-trivial solutions is given as follows:

$$[(\epsilon_1 + \epsilon_2)\epsilon_1 + \epsilon_3)]/[(\epsilon_1 - \epsilon_2)(\epsilon_1 - \epsilon_3)] = e^{-4kd}. \tag{10}$$

A similar dispersion relation has been obtained for surface polaritons by solving macroscopic Maxwell's equations. Here equation (10) is derived on the basis of microscopic theory for the polarization field of relative displacements of ions without coupling with photons. Only the electric field due to a coulombic interaction is considered, since we confine ourselves to electron–phonon coupling in the present work.

Equation (10) gives four branches of frequencies as functions of the 2D wavenumber, k. We denote them by $\omega_\xi(\xi = 1,2,3,4)$. Generally, the frequencies should be obtained numerically. We will discuss them later.

The normalized eigenvector for the mode of frequency ω_ξ can be solved as

$$\Phi_\xi(k,z)=\begin{cases}\eta_2 A_\xi(\beta_2 e^{-kz},\ i\beta_2 e^{-kz}) & (z>d)\\ \eta_1 A_\xi(e^{kz}+\beta_1 e^{-kz},\ -ie^{kz}+i\beta_1 e^{-kz}) & (|z|\leqslant d)\\ \eta_3 A_\xi(\beta_3 e^{kz},\ -i\beta_3 e^{kz}) & (z<-d)\end{cases} \tag{11}$$

where

$$\begin{aligned}\beta_1&=e^{2kd}(\epsilon_1+\epsilon_2)/(\epsilon_1-\epsilon_2)\\ \beta_2&=2e^{2kd}\epsilon_1(\epsilon_2-1)/[(\epsilon_1-1)(\epsilon_1-\epsilon_2)]\\ \beta_3&=2\epsilon_1(\epsilon_3-1)/[(\epsilon_1-1)(\epsilon_1+\epsilon_3)]\end{aligned} \tag{12}$$

and

$$\begin{aligned}\eta_\lambda&=(\epsilon_\lambda-\epsilon_{\infty\lambda})/[\omega_{T\lambda}(\epsilon_{0\lambda}-\epsilon_{\infty\lambda})^{1/2}(\epsilon_\lambda-1)]\\ A_\xi&=\{k/[2(I_1+I_2+I_3)]\}^{1/2}\end{aligned} \tag{13}$$

with

$$I_1=\eta_1^2(1+\beta_1^2)\sinh(2kd)\qquad I_2=\tfrac{1}{2}\eta_2^2\beta_2^2e^{-2kd}\qquad I_3=\tfrac{1}{2}\eta_3^2\beta_3^2e^{-2kd}.$$

It will turn out later that these modes are localized in the vicinities of the interfaces and then we call them IO modes.

3. Electron–IO-phonon interaction Hamiltonian

We now go on to derive the electron–IO-phonon interaction Hamiltonian. To this end we first quantize the polarization field of lattice vibrations.

By using a standard quantization procedure, one can write u and E as quantum field operators. The contribution of the IO phonons to the relative displacement of the ion pair at r has the following form:

$$u(r)=\sum_{k\xi}\left(\frac{\hbar}{2Sn\mu\omega_\xi}\right)^{1/2}e^{ik\cdot\rho}\Phi_\xi(k,z)a_{k\xi}+\text{HC} \tag{14}$$

where $a^+_{k\xi}(a_{k\xi})$ is the Bose creation (annihilation) operator of the IO phonon of frequency ω_ξ and 2D wavenumber k and satisfies the commutation relations for Bose operators. On the other hand, we have the following relations for the relative displacement and the local field:

$$E^l(r)=\{[ne^*(4\pi/3+\gamma_k)]/[1-n\alpha(4\pi/3+\gamma_k)]\}u(r) \tag{15}$$

from (2), (9) and the well known Lorentz relation

$$E^l=(4\pi/3+\gamma_k)P. \tag{16}$$

Substituting equations (14) and (15) into the free-polarization Hamiltonian

$$H_F = \int d\boldsymbol{r}\, \frac{n\mu}{2}(\dot{u}^2 + \omega_0^2 u^2) - \int d\boldsymbol{r}\, \frac{ne^*}{2} \boldsymbol{E}^l \cdot \boldsymbol{u} \tag{17}$$

we can obtain the free IO-phonon field Hamiltonian

$$H_{IO} = \sum_{k\xi} \hbar\omega_\xi (a^+_{k\xi} a_{k\xi} + \tfrac{1}{2}). \tag{18}$$

The interaction between an electron at $\boldsymbol{r}$ and a polarization field can be written as the following well known form

$$H_{e-p} = \int e \frac{\boldsymbol{r}' - \boldsymbol{r}}{|\boldsymbol{r}' - \boldsymbol{r}|^3} \cdot \boldsymbol{P}(\boldsymbol{r}')\, d\boldsymbol{r}'. \tag{19}$$

Moreover, the polarization field associated with the displacement $\boldsymbol{u}(\boldsymbol{r})$ can be written as

$$\boldsymbol{P}(\boldsymbol{r}) = \{ne^*/[1 - n\alpha(4\pi/3 + \gamma_k)]\}\boldsymbol{u}(\boldsymbol{r}) \tag{20}$$

from equations (2) and (16).

Putting equations (14), (19) and (20) together with equations (4), (8) and (9) and using a Fourier transform

$$\frac{\boldsymbol{r}' - \boldsymbol{r}}{|\boldsymbol{r}' - \boldsymbol{r}|^3} = -\int d\boldsymbol{k}\, e^{i\boldsymbol{k}\cdot(\boldsymbol{\rho}' - \boldsymbol{\rho})} \frac{i\boldsymbol{K}}{2\pi k} e^{-k|z' - z|} \tag{21}$$

the Fröhlich-like Hamiltonian for the electron–IO-phonon interaction is finally obtained as

$$H_{e-IO} = \sum_{k\xi} G_\xi(\boldsymbol{k}, z) e^{i\boldsymbol{k}\cdot\boldsymbol{\rho}} a_{k\xi} + \text{HC}. \tag{22}$$

In this equation the coupling function G_ξ is given by the integral

$$G_\xi(\boldsymbol{k}, z) = i \sum_\lambda \int_{(\lambda)} dz'\, h_0 \eta_\lambda^{-1} e^{-k|z' - z|} \frac{\boldsymbol{K}^*}{k} \cdot \Phi_\xi(\boldsymbol{k}, z'). \tag{23}$$

Completing the integral in equation (23) we have

$$G_\xi(\boldsymbol{k}, z) = \begin{cases} iC^{II} e^{-kz} & (z > d) \\ i(C_1^I e^{kz} + C_2^I e^{-kz}) & (|z| \leqslant d) \\ iC^{III} e^{kz} & (z < -d) \end{cases} \tag{24}$$

where

$$\begin{aligned} C_1^I &= A_\xi[h_0(1 - \beta_1 e^{-2kd}) + h_0\beta_2 e^{-2kd}]/k \\ C_2^I &= A_\xi[h_0(\beta_1 - e^{-2kd}) + h_0\beta_3 e^{-2kd}]/k \\ C^{II} &= A_\xi[2h_0 \sinh(2kd) + h_0\beta_2 + h_0\beta_3 e^{-2kd}]/k \\ C^{III} &= A_\xi[2h_0\beta_1 \sinh(2kd) + h_0\beta_2 e^{-2kd} + h_0\beta_3]/k \end{aligned} \tag{25}$$

and

$$h_\lambda = [\pi\hbar e^2/(2S\omega_\xi)]^{1/2}. \tag{26}$$

It is obvious that the coupling functions are spatially and wavenumber dependent. The interface localization of the IO modes can be also found from the spatial dependence of the corresponding electron–phonon coupling. It is seen from equation (24) that the coupling intensities of the electron with the IO phonons have their maxima at the interfaces $z = d$ and $z = -d$ and decrease as the electron moves away from the interfaces. The larger the well width or the wavenumber, the more noticeable the interface localization.

As for the wavenumber dependence, the electron–phonon coupling decays rapidly with increasing wavenumber. Therefore the contribution of the IO phonons of smaller wavenumbers to the electron–phonon coupling is dominant, i.e. only the phonon modes in the vicinity of the centre of the Brillouin zone (BZ) are important. This is also expected in our continuum approximation. The above-mentioned properties of IO modes will be clearly indicated by the following numerical results for several practical systems.

4. Analysis of special cases

Before doing the numerical computations we discuss briefly some special cases.

4.1. Large- and small-wavenumber limits

In understanding the character of the IO modes it is worth discussing the extreme cases of large and small k respectively.

(i) *Large-wavenumber limit, i.e.* $k \to \infty$. In this case the IO polarization wavelengths are much smaller than the well width and the interfaces can be considered to be isolated from each other. So the mode frequencies become those of the individual interfaces given by $\epsilon_1 + \epsilon_2 = 0$ and $\epsilon_1 + \epsilon_3 = 0$. Since the barrier materials 2 and 3 are different, the four branches of the IO frequencies do not reduce to two branches at $k \to \infty$. This behaviour is far from that observed in a symmetric quantum well [11, 13].

Furthermore the electron–IO-phonon coupling functions tend to zero in this limit. This is the natural behaviour of the electron–phonon coupling for either bulk or interface modes because of the coulombic interaction.

(ii) *Small-wavenumber limit, i.e.* $k \to 0$. In the limit of small wavenumber, the frequencies reduce to $\omega_1 = \omega_{T1}$, $\omega_2 = \omega_{L1}$, but ω_3 and ω_4 are given by $\epsilon_2 + \epsilon_3 = 0$. The results are again different from those in symmetric double heterostructures. The coupling between two different barrier materials is considerable.

The eigenvectors and coupling functions of the modes of frequencies ω_{T1} and ω_{L1} have the simple forms

$$\Phi_1(0, z) = \begin{cases} [1/(2d)^{1/2}](1, 0) & |z| \leqslant d \\ 0 & \text{otherwise} \end{cases} \tag{27}$$

$$G_1(0, z) = ih_0(2d)^{1/2}\eta_1^{-1} \qquad \text{everywhere} \tag{28}$$

for the mode of ω_{T1}, i.e. the TO-frequency mode, and

$$\Phi_2(0,z) = \begin{cases} [1/(2d)^{1/2}](0,-\mathrm{i}) & |z| \leqslant d \\ 0 & \text{otherwise} \end{cases} \tag{29}$$

$$G_2(0,z) = \begin{cases} \mathrm{i}h_0(2d)^{1/2}\eta_1^{-1} & z > d \\ \mathrm{i}h_0(2/d)^{1/2}z\eta_1^{-1} & |z| \leqslant d \\ -\mathrm{i}h_0(2d)^{1/2}\eta_1^{-1} & z < -d \end{cases} \tag{30}$$

for the mode of ω_{L1}, i.e. the LO-frequency mode.

It is found from equations (27) and (29) that the IO modes for such a small-wavevector limit are confined in the well. Moreover, the TO-frequency mode is longitudinal ($\boldsymbol{P}_1 \| \boldsymbol{k}$) while the LO-frequency mode is transverse ($\boldsymbol{P}_2 \perp \boldsymbol{k}$). This is somewhat like the bulk-like slab modes in the well material. However, the IO modes at the TO and LO frequencies are both accompanied by microscopic fields and coupled with electrons either inside or outside the well.

4.2. Special systems

(i) *Symmetric quantum well.* Putting $\epsilon_2 = \epsilon_3$ we obtain exactly the same results as for a symmetric quantum well. The results are the same as those given in previous papers [10, 12].

(ii) *Single heterojunction.* Putting ϵ_2 (or ϵ_3) equal to one, i.e. supposing material 2 (or 3) to be a vacuum, we get a film on a thick substrate. This is a kind of single heterojunction problem. In this case the implied dispersion relation for $\epsilon_2 = 1$ becomes

$$[(\epsilon_1 + \epsilon_3)(\epsilon_1 + 1)]/[(\epsilon_1 - \epsilon_3)(\epsilon_1 - 1)] = \mathrm{e}^{-4kd}. \tag{31}$$

The IO modes reduce to three branches. The corresponding changes for the eigenvectors and coupling functions are also made at the same time. Putting $d = 0$ we get a single interface between 2 and 3 at $z = 0$. The dispersion relation is given by

$$\epsilon_2 + \epsilon_3 = 0. \tag{32}$$

The results are the same as those obtained by previous authors [10].

5. Numerical results and discussion

For ease of representation we have computed numerically the dispersion relations, eigenvectors and electron–IO-mode coupling functions for several particular systems. The results are given as follows.

Table 1. Characteristic parameters used in the numerical calculation. Energy is measured in meV.

	GaAs[a]	$In_{0.15}Ga_{0.85}As$[b]	$In_{0.47}Ga_{0.53}As$[c]	$Al_{0.15}Ga_{0.85}As$[a]	$Al_{0.3}Ga_{0.7}As$[a]	InP[d]
$\hbar\omega_{LO}$	36.25	32.24	33.54	35.31	34.45	42.78
$\hbar\omega_{TO}$	33.29	29.00	31.49	33.17	32.99	37.65
ϵ_∞	10.89	11.03	11.32	10.48	10.07	9.56

[a] [18].
[b] [19].
[c] [20].
[d] [21].

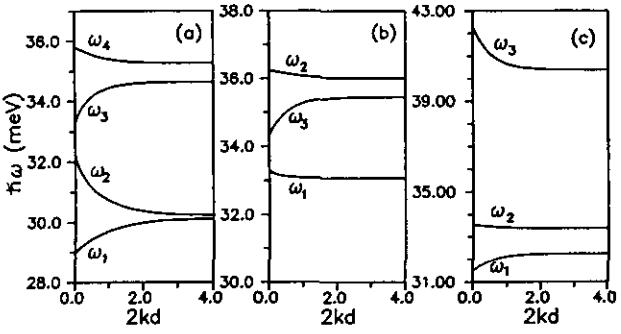

Figure 2. Phonon energies of the 10 modes as functions of the wavenumber k in (a) a $GaAs/In_{0.15}Ga_{0.85}As/Al_{0.15}Ga_{0.85}As$ single quantum well; (b) a $GaAs/Al_{0.3}Ga_{0.7}As$ single heterojunction; (c) an $In_{0.47}Ga_{0.53}As/InP$ single heterojunction. Phonon energy is measured in meV and length in $2d$.

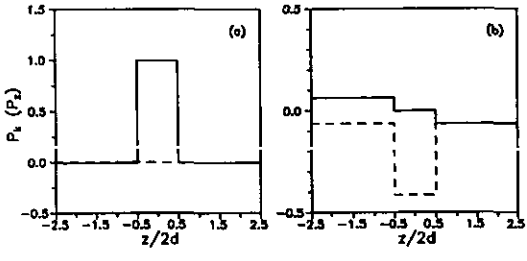

Figure 3. k-components (solid line) and z-components (dashed line) of the eigenvectors of (a) $\hbar\omega_1 = 29.01$ meV and (b) $\hbar\omega_2 = 32.19$ meV as functions of $z/2d$ at $2kd = 0.01$ for the system in figure 2(a).

5.1. GaAs/InGaAs/AlGaAs single quantum well

Equation (10) has been solved numerically for a $GaAs/In_{0.15}Ga_{0.85}As/Al_{0.15}Ga_{0.85}As$ single quantum well. The material parameters used in the computations are listed in table 1. The numerical results for the phonon energies $\hbar\omega_\xi$ of the 10 modes as functions of the 2D wavenumber k are plotted in figure 2(a). It is clear that there exist four branches of the 10 phonons supported by two interfaces. In contrast to those in a symmetric quantum well, these modes are neither symmetric nor antisymmetric. Their frequencies do not reduce to two branches at $k \to \infty$.

Figure 3 shows the components along the k- and z-directions of the eigenvectors whose frequencies are close to ω_{TI} and ω_{LI} respectively at $k = 0.01/2d$. The modes are almost confined to the well material and again the longitudinal mode is near the

bulk TO frequency, but the transverse mode is near the LO frequency.

The wavenumber and spatial dependences of the electron–IO-phonon coupling functions are illustrated in figure 4, (*a*) and (*b*), for $z = d$ and $k = 0.01/2d$ respectively. Figure 4 shows that the coupling functions are localized in the interface and important at the small wavenumbers in the vicinity of the centre of the BZ.

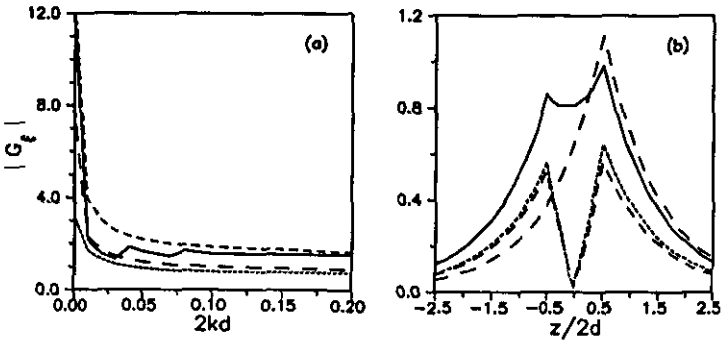

Figure 4. Absolute values of the coupling functions for the four branches of IO modes as functions of (*a*) wavenumber k at $z \approx d$ and (*b*) well width z at $k = 0.01$ with $2d = 1$ and $(\pi e^2 \hbar \omega_{T1}/2)^{1/2} = 1$ for the system in figure 2(*a*).

5.2. Heterojunctions

We have considered the single-heterojunction system in which a film lies on a thick substrate. There are three branches of IO modes in this kind of system. The numerical results for the phonon energies of IO modes in the GaAs/AlGaAs and InGaAs/InP heterojunction system are shown in figure 2, (*b*) and (*c*) respectively. The frequencies start at the values $\omega_1 = \omega_{T1}$, $\omega_2 = \omega_{L1}$ and ω_3 given by $\epsilon_3 + 1 = 0$ at $k = 0$ and then tend to the frequencies given by $\epsilon_1 + \epsilon_3 = 0$ and $\epsilon_1 + 1 = 0$ at $k \to \infty$.

Our numerical computations for the two systems show that in the vicinity of the centre of the BZ, the eigenmodes of the frequencies close to the TO and LO frequencies are again almost confined to the film and have an interchange of longitudinal and transverse characteristics. Both of them couple with the electrons in the systems. The characteristics of the curves describing the eigenvectors and coupling functions in the heterostructures are quite similar to those in figures 3 and 4, so we do not plot them here.

In summary we have investigated the interface optical modes in a general double-heterojunction system on the basis of the dielectric continuum model. The Hamiltonian for the electron–IO-phonon interaction in the system was derived. It was found that there exist four branches of IO polarization modes coupled with the electrons in the system. In contrast to what is found for symmetric double heterostructures, the four branches of the IO frequencies do not reduce to two branches at $k \to \infty$. The contribution of small-wavevector phonons to the electron–phonon coupling is dominant. In the vicinity of the centre of the BZ, the IO modes with the bulk TO and LO frequencies of the well material are localized inside the well. However, the properties of these modes are far from those of bulk-like modes. An interchange of longitudinal- and transverse-phonon characteristics corresponding

to the TO and LO frequencies is also found theoretically for IO modes. Both the TO and LO phonons couple with the electrons in the system. It was demonstrated by our theoretical calculation that the Fröhlich interaction between an electron and the IO phonons is important for electron–phonon scattering in heterostructures. In general the contribution of IO-mode coupling will lower the resonant frequencies. A more detailed calculation for polaron effects in heterostructures should be done in order to interpret satisfactorily the experimental phenomena. The electron–IO-phonon interaction Hamiltonian derived here can be used in studying polaron problems for heterostructures. Further work is in progress.

Finally, it is to be noted that the optical modes of a ternary mixed crystal, such as AlGaAs etc., have two-mode character [18, 22]. Only a main mode coupled strongly with the electrons is considered in our numerical calculation. This is incomplete but does not change the essential characteristics of the IO modes.

References

[1] Klein M V 1986 *IEEE J. Quantum Electron.* **QE-22** 1760
[2] Zucker J E, Pinczuk A, Chemla D S, Gossard A and Wiegmann W 1984 *Phys. Rev. Lett.* **53** 1280
[3] Ziesmann M, Heitmann D and Chang L L 1987 *Phys. Rev.* B **35** 4541
[4] Brummell M A, Nicholas R J, Hopkins M A, Harris J J and Foxon C T 1987 *Phys. Rev. Lett.* **58** 77
[5] Nicholas R J, Brunel L C, Huant S, Karrai K, Portal J C, Brummell M A, Razeghi M, Cheng K Y and Cho A Y 1985 *Phys. Rev. Lett.* **55** 883
[6] Cardona M 1989 *Superlatt. Microstruct.* **5** 27
[7] Lassnig R 1984 *Phys. Rev.* B **30** 7132
[8] Das Sarma S 1986 *Phys. Rev. Lett.* **57** 651
[9] Peeters F M, Warmenbol P and Devreese J T 1990 *Europhys. Lett.* **12** 435
[10] Ushioda S 1981 *Progress in Optics* vol XIX ed E Wolf (Amsterdam: North-Holland) p 139
[11] Mori N and Ando T 1989 *Phys. Rev.* B **40** 6175
[12] Wendler L 1985 *Phys. Status Solidi* b **129** 513
[13] Liang X X and Wang X 1991 *Phys. Rev.* B **43** 5155
[14] Born M and Huang K 1954 *Dynamical Theory of Crystal Lattices* (Oxford: Clarendon)
[15] Fuchs R and Kliewer K L 1965 *Phys. Rev.* **140** A2076
[16] Lucas A A, Kartheuser E and Badro R G 1970 *Phys. Rev.* B **2** 2488
[17] Licari J J and Evrard R 1977 *Phys. Rev.* B **15** 2254
[18] Adachi S 1985 *J. Appl. Phys.* **58** R1
[19] Lucovsky G and Chen M F 1970 *Solid State Commun.* **8** 1397
[20] Pearsall T P, Charles R and Portal J C 1983 *Appl. Phys. Lett.* **42** 436
[21] Kartheuser E 1972 *Polarons in Ionic Crystals and Polar Semiconductors* ed J T Devreese (Amsterdam: North-Holland)
[22] Wang X and Liang X X 1990 *Phys. Rev.* B **42** 8915